Biointerphases (2012) 7:57
DOI 10.1007/s13758-012-0057-3

ARTICLE

Computer Simulation of Water-Mediated Adhesion Between Phospholipid Bilayer and Solid Support Functionalized with Self-Assembled Monolayers

Alexander Pertsin · Michael Grunze

Received: 17 May 2012 / Accepted: 16 August 2012 / Published online: 28 August 2012

Abstract An attempt is made to estimate, via computer simulation of the force–distance relation, the free energy of adhesion between a phosphatidylethanolamine bilayer and an alkanethiolate self-assembled monolayer (SAM) in aqueous medium. The simulations are performed using the grand canonical Monte Carlo technique and atomistic force fields. The bilayer adhesion free energy is predicted to be -22 ± 3 mJ/m^2 (–1.4 ± 0.2 kcal/mol) on a hydrophilic carboxyl-terminated SAM and -1 ± 1 mJ/m^2 (–0.06 ± 0.06 kcal/mol) on a hydrophobic methyl-terminated SAM.

In the last two decades, the water-mediated interaction of lipid bilayers with various surfaces has received much attention [1]. This is explained, in particular, by ever-increasing practical interest in planar bilayer membranes supported on solid substrates. For biologists and biophysicists, the supported lipid bilayers (SLBs) provide a good model system for studying the membrane structure and properties because of a better stability of SLBs with respect to chemical manipulation and destructive effects of surface-sensitive characterization techniques. For physicists and physicochemists, SLBs are of interest mainly as a means for biofunctionalization of inorganic solids and polymeric materials. A practical outcome of the associated research is the development of new biosensors, which combine the small thickness and high electrical resistivity of SLBs with their ability to serve as a matrix for incorporating receptors and, simultaneously, to suppress non-specific ligand binding [1].

A. Pertsin (✉) · M. Grunze
Angewandte Physikalische Chemie, Universität Heidelberg,
Im Neuenheimer Feld 253, 69120 Heidelberg, Germany
e-mail: ig3@ix.urz.uni-heidelberg.de

A critical parameter that governs the stability and other properties of SLBs is the free energy of adhesion between the bilayer and substrate, W. In a general case, W can be represented as the sum of two basic components. One component is due to direct bilayer–substrate interactions, while the other arises from so-called hydration forces. These latter are associated with a thin aqueous film that is usually present between the bilayer and substrate. (It is this film that maintains the lateral fluidity of the bilayer.) In principle, W can be determined experimentally by the surface force apparatus (SFA) or atomic force microscopy (AFM) and related techniques. A thorough inspection of the literature has however revealed only one relevant study, as recently reported by Anderson et al. [2] from the Israelachvili group for zwitterionic phospholipid bilayers (DMPC) supported on silica glass substrates.

The lack of experimental data on the bilayer-substrate adhesion energy attracts attention to computer simulations as a potential means of adequately modeling SFA experiments based on realistic force fields. An advantage of computer simulations is the possibility of partitioning W into individual physical components corresponding to the individual components of the intermolecular interaction energy. The knowledge of the physical components of W offers a clearer insight into the mechanism of the bilayer–substrate adhesion.

By now, the number of computer simulations of SLBs is very limited. Of the eight published simulation studies [3–10], only three [3–5] were based on a realistic atomistic description. The others were concerned with oversimplified coarse-grained [6–8] and highly coarse-grained [9, 10] models, which are hardly capable of quantitatively describing water-mediated bilayer–substrate interactions. Of particular interest is the atomistic simulation study by Heine et al. [3] who made a first attempt to quantify the

adhesion energy between a lipid bilayer and α-quartz substrate in aqueous media. Although the simulation correctly predicted the equilibrium separation between the bilayer and substrate, the calculated adhesion energies proved to be about two orders of magnitude higher than the experimental values measured by Anderson et al. [2] (0.5–1.0 mJ/m^2, depending on the method of bilayer preparation).

It is worth noting that the above-cited computer simulations of SLBs were all performed using the molecular dynamics (MD) technique and closed statistical ensembles (*NVT* and NP_NT), where the number of particles in the confined system remained constant. By contrast, a real SLB studied in an SFA experiment represents an *open* confined system, where water sandwiched between the bilayer and substrate is allowed to exchange molecules with a surrounding bulk water reservoir. The relevant statistical description is provided by the grand canonical (μVT) or isostress (μP_NT) ensembles.

In our previous simulations of the water-mediated interaction between two identical phospholipid bilayers [11, 12], the problem of modeling an open system was solved by resorting to a grand canonical Monte Carlo (GCMC) technique involving special expedients for enhancing sampling efficiency [13]. The aim was to understand the physical nature of forces responsible for the short-range interbilayer repulsion. In the present work, our GCMC simulations are extended to asymmetric systems, where one bilayer is replaced by a solid substrate. Unlike the previous studies [11, 12], now the interest is concentrated on separations where one can expect bilayer–substrate attraction responsible for adhesion.

The specific lipid considered in the present work is dilauroylphosphatidylethanolamine (DLPE) studied in our previous simulations [11, 12]. As a substrate, we use a gold support functionalized by carboxyl- and methyl-terminated alkanethiolate self-assembled monolayers (hereafter, O-SAM and C-SAM) of the general formula $X(CH_2)_nS$ (X = COOH and CH_3, $n = 12$ and 13, respectively). This choice is natural as far as aqueous medium is concerned, where the water affinity of the substrate may play a decisive role in the bilayer–substrate adhesion.

As a preliminary stage of this work, we have recently simulated water-mediated adhesion between the O- and C-SAMs both in symmetric and asymmetric combinations (i.e., between like SAMs and between unlike SAMs, respectively) [14]. The calculated free energies of adhesion proved to be in acceptable agreement with the available experimental data extracted from AFM measurements of force–distance relations. The behavior of the two symmetric and one asymmetric systems with increasing confinement was quite different. The symmetric system bounded by the hydrophilic O-SAMs kept confined water at all separations tried, including separations in the region of repulsive pressures. The system confined by two hydrophobic C-SAMs showed a capillary evaporation occurring at a fairly large separation in the attractive region. As a consequence, the adhesion energy was mainly determined by the direct interaction of bare SAMs. A capillary evaporation was also observed in the asymmetric O-SAM/water/C-SAM system. In this case, however, the evaporation was incomplete. The remaining water molecules were all adsorbed on the hydrophilic O-SAM, while the hydrophobic C-SAM was separated from the rest of the system by a thin vapor layer. These observations have provided a good basis for a comparative analysis of the behavior of DLPE/water/SAM systems.

The model system used in the present simulations reflects the configuration of an SFA experiment, as schematically depicted in Fig. 1. The system elements shown in black are explicitly present in the system, while those shown in gray are simulated implicitly. As in our previous studies [11, 12] the outer (upper) phospholipid monolayer was represented in a mean-field manner as a flat structureless surface interacting with the carbon atoms of the lower monolayer through a (3–9) inverse power potential. The position of this surface corresponds to the mid-plane of the bilayer, as shown by the dashed line in Fig. 1. The parameters of the (3–9) potential were calibrated so as to fit atomistic force field results for the interaction energy of two DLPE monolayers facing each other with their hydrophobic sides. The inter- and intramolecular energies of DLPE were calculated using the AMBER-based force field refined by Smondyrew and Berkowitz [15]. The methyl and methylene groups were treated in the united-atom approximation, while the hydrogen atoms of the amino group were treated explicitly. The DLPE molecules were regarded as flexible but subject to bond-length constraints. These latter were

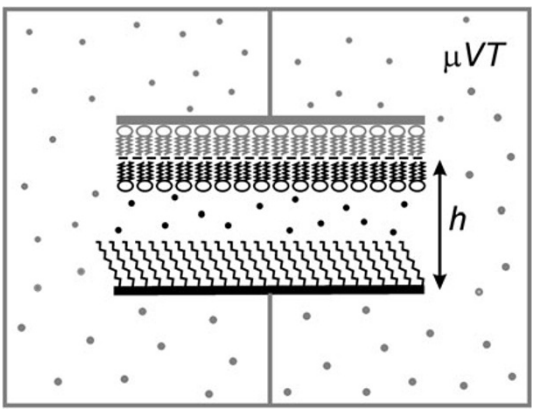

Fig. 1 Configuration of the simulation model. The parts simulated explicitly and implicitly are shown in *black* and *gray*, respectively

implemented using the rotational displacement procedure suggested in our early paper [16].

The gold support was represented by a two-dimensional hexagonal lattice of force sites corresponding to the (111) plane of the gold monocrystal. The interaction of gold with water was neglected. The alkane chains were described with an all-atom model, with the atom–atom potentials calibrated by Williams [17] by fitting the equilibrium structure and lattice energy of hydrocarbon crystals to the relevant experimental data. The potential parameters of sulfur were the same as used by Mar and Klein [18] in their MD simulations of an alkanethiolate SAM, while the interactions involving the COOH group were treated using the respective potentials from the OPLS-AA force field [19]. As with DLPE, the conformation of the SAM molecules was subject to bond-length constraints.

In calculations of the intermolecular interaction energy, each molecule bearing Coulombic charges was represented as a set of electrically neutral groups. At short separations between the group centers, the electrostatic interaction energy was calculated directly as the sum of charge–charge interactions, while at large separations the dipole–dipole group–group approximation was used. The cutoff distances for the charge–charge and dipole–dipole contributions were 20 and 100 Å, respectively. The Lennard–Jones potentials describing the exchange repulsion and dispersion interactions were cut off at a distance of 15 Å.

The bulk water reservoir surrounding the SLB in Fig. 1 was treated implicitly by equating the chemical potential of confined water to that of bulk water [20, 21], as determined in separate GCMC simulations of the latter. The fluctuations of the number of confined water molecules were simulated through repeated attempts to create or destruct a water molecule in the confined region. The water–water interactions were described with the TIP4P force field [22], while the mixed water—DLPE and water—SAM interaction parameters were calculated using geometric mean combination rules.

The substrate (SAM) side of the simulation box was constructed based on an orthorhombic unit cell with two symmetrically distinct alkanethiolate molecules and periods $a = 3c$, $b = c\sqrt{3}$ where $c = 4.08$ Å is the lattice constant of gold. The starting arrangement of the molecules in the unit cell was taken the same as found in our early work [23] by global energy minimization. The simulation box was composed of 18 unit cells (3 unit cells along x axis and 6 unit cells along y), so that the number of alkanethiolate molecules in the substrate side of the simulation box was 36 and the lateral dimensions of the simulation box were $L_x = 3a = 36.72$ Å, $L_y = 6b = 42.4$ Å.

The starting configuration of the lipid side of the simulation box was built up proceeding from the crystal-state bilayer configuration, as observed in the DLPE–acetic acid crystal [11]. To make the lipid and substrate sides of the system commensurable, the crystal-state bilayer configuration was slightly stretched along the x axis and compressed along the y axis so as to fit the lateral dimensions of the simulation box. The area per lipid molecule in the resulting configuration proved to be 48.7 Å^2, which is close to a semi-empirical estimate of 51.2 Å^2 reported by Nagle and Wiener [24] for fluid-phase DLPE bilayers at 308 K.

The GCMC simulation procedure used was discussed in detail elsewhere [11, 12]. In brief, the simulations were performed with a fixed number of the bilayer and substrate molecules, so that the system was actually treated as a semi-grand canonical ensemble. A total of five types of random moves were attempted: insertion, deletion, and translational-rotational (hereafter displacement) moves of water plus conformational and displacement moves of DLPE and SAM molecules. To improve the acceptance probability of insertion and deletion moves, the Swendsen–Wang filtering [25] and an orientational bias procedure [26] were used. The former rejected an improbable insertion or deletion of a randomly selected water molecule based on its position and a computationally cheep predictor of the associated energy. The latter did the same with respect to molecular orientation. The attempts to insert a water molecule were made over the whole volume treated explicitly.

The key quantity evaluated in our GCMC simulations was the normal pressure, p. It was calculated in the "force form" (as opposed to the "virial form") by summation of the z-components of the forces exerted on the DLPE bilayer by the SAM substrate and water. The total pressure p was represented as the sum two components, $p = p_d + p_h$, where p_d was associated with direct bilayer–substrate interactions and p_h was the so-called hydration (solvation) pressure [14] due to the forces exerted on the bilayer by water molecules. (It is worth noting in this context that the hydration pressure p_h is frequently used to mean the total pressure p operating between the substrates. Here we prefer to follow the definition given by Evans and Markoni [27], where p_h is just a component of p.)

The direct pressure p_d was further partitioned into contributions from electrostatic, dispersion, and exchange repulsion (steric) forces, $p_d = p_d^{elst} + p_d^{disp} + p_d^{rep}$, by collecting the forces associated with the respective terms of the intermolecular interaction potentials.

The adhesion free energy was calculated by integrating the pressure-separation relation $p(h)$ from the equilibrium separation, h_0, as defined by the condition $p(h_0) = 0$, to the largest separation tried, h_{max}, where the magnitude of p was within the respective statistical error. All the simulations were performed at a temperature of 308 K.

Considering a fairly slow convergence of pressure [14], we had to use very long GCMC runs and to check the reproducibility of the calculated values of pressure by comparing the results of independent runs differing in the initial structure and/or the sequence of random numbers. The length of a GCMC run was 2×10^6 passes, each comprising N_0 moves, where N_0 is the initial number of water molecules in a given pass. The first half of the run served to equilibrate the system, while the ensemble averages were calculated in the second half. For each particular separation h, 5–7 independent GCMC runs were performed and the calculated quantities were averaged out. The calculation error was estimated as the average absolute deviation from the mean. Typical curves demonstrating the convergence of pressure in the course of five independent GCMC runs are presented in Fig. 2.

We first consider the case of the hydrophilic O-SAM substrate. The calculations of the pressure-separation relation $p(h)$ were performed in order of increasing confinement starting from $h_{max} = 43.5$ Å, where the magnitude of p did not exceed the respective average deviation, Δ_p. The highest confinement tried for at $h = 33$ Å, which corresponded to strongly repulsive bilayer–substrate interaction. The calculated $p(h)$ is shown in Fig. 3a, where positive and negative pressures correspond to repulsion and attraction, respectively. The curve shows a well defined minimum at $h = 36$ Å with a depth of about 0.7 kbar. The equilibrium separation is at $h_0 \approx 34.3$ Å. The hydration degree at the separation nearest to h_0 ($h = 34.5$ Å) is 6.6. The integration of $p(h)$ from 34.3 to 43.5 Å results in the adhesion free energy $W = -2.2 \pm 0.3$ kbar Å $= -22 \pm 3$ mJ/m^2, which is close to the values calculated for the O-SAM/water/O-SAM and O-SAM/water/C-SAM systems (-26 ± 4 and -25 ± 3 mJ/m^2, respectively) [14].

The distribution of pressure over its individual components at the separation of strongest attraction (36 Å) is shown in Fig. 4a. It can be seen that the factor responsible for adhesive attraction is the direct bilayer–substrate interaction p_d, which is in turn determined by the interplay between the attractive p_d^{elst} and p_d^{disp}, on one hand, and strongly repulsive p_d^{rep}, on the other. It is worth noting that the force field used in our simulations involves no explicit terms responsible for hydrogen bonding. The latter is described by the electrostatic interaction of proton-donor and proton-acceptor groups, and hence the contribution to p_d due to formation of hydrogen bonds between the bilayer and substrate enters into p_d^{elst}, while the contribution to pressure from hydrogen bonds formed by water with the bilayer and substrate is a part of p_h. As seen from Fig. 4a, the hydration forces play an important role in the total force balance: Being comparable in magnitude with p_d, the repulsive p_h substantially weakens the water-mediated adhesion between the bilayer and substrate.

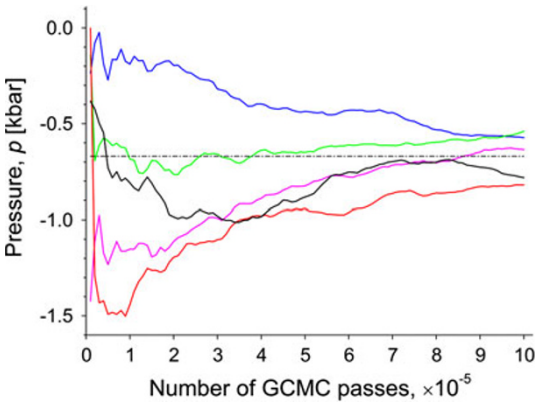

Fig. 2 Convergence of pressure in the course of five independent GCMC runs. The data refer to the DLPE/water/O-SAM system at $h = 36$ Å

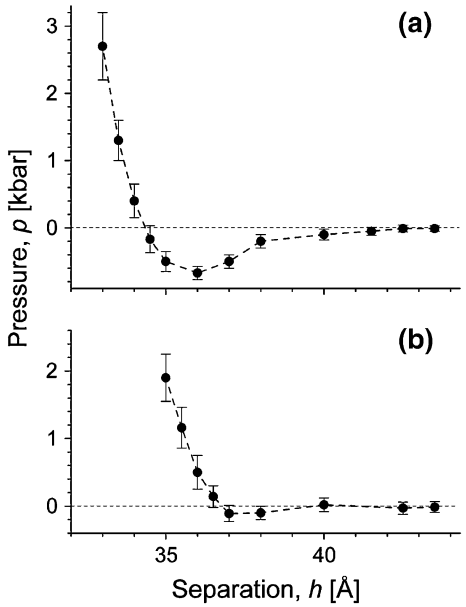

Fig. 3 Pressure-separation relations for DLPE bilayer supported on O-SAM (**a**) and C-SAM (**b**)

The replacement of the hydrophilic O-SAM substrate by the hydrophobic C-SAM reduces the adhesive strength to values comparable with the calculation error (Fig. 3b). The minimum of the $p(h)$ curve occurs somewhere between 37 and 38 Å and has a depth of about 0.1 ± 0.1 kbar. The equilibrium separation h_0 is at $h = 36.8$ Å. The hydration degree at the separation nearest to h_0 ($h = 37$ Å) is 7.2. The distribution of pressure over its components (Fig. 4b) is qualitatively similar to that found in the DLPE/water/O-SAM system, except for the lack of p_d^{elst} because of the absence of electrostatic terms in the Williams potentials [17].

The adhesion free energy W calculated from the $p(h)$ curve in Fig. 3b is -1 ± 1 mJ/m^2. The corresponding

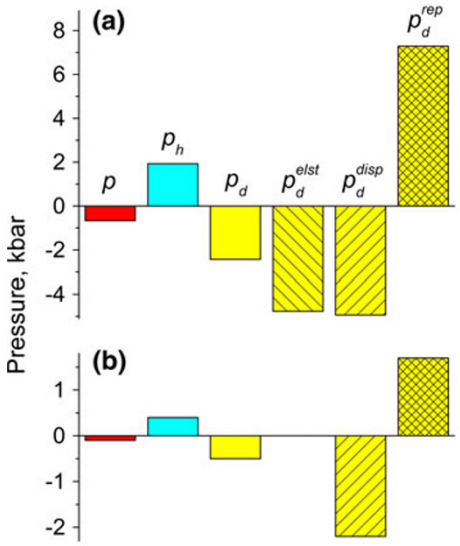

Fig. 4 Distribution of pressure over its physical components for DLPE supported on O-SAM (**a**) and C-SAM (**b**) at separations corresponding to the minimum of the pressure-separation curve. Note that the pressure scales in **a** and **b** are different

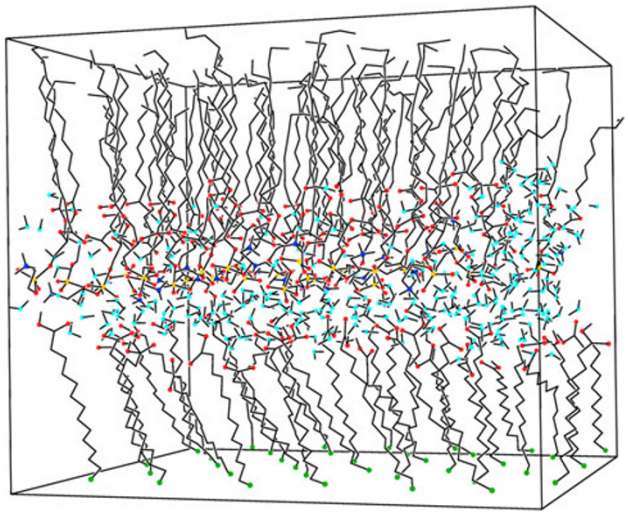

Fig. 5 Snapshot of the DLPE/water/O-SAM system at $h = 36$ Å. O, N, and P atoms of DLPE are shown in *red, blue,* and *purple*, respectively; S and O atoms of SAM are shown in *green* and *red*; water O atoms are shown in *turquoise*

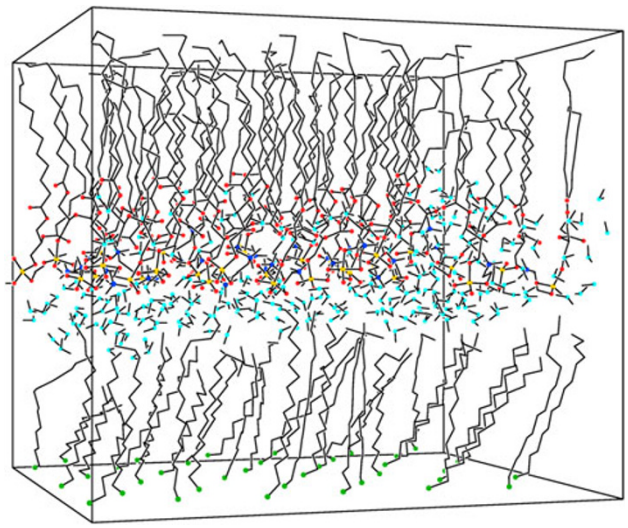

Fig. 6 Snapshot of the DLPE/water/C-SAM system at $h = 37$ Å

experimental value of W is not available because the attempts to prepare an SLB by adsorption of small unilamellar vesicles (SUV) onto C-SAM failed [28, 29]: The SUV adsorption led to formation of a supported lipid monolayer (SLM) with the hydrophobic tails directed toward the hydrophobic SAM substrate. The associated adhesion energy has not been measured experimentally but it hardly differs significantly from the value of -88 ± 35 mJ/m^2 found in AFM experiments with the C-SAM/water/C-SAM system [30]. That is, the contact of the hydrophobic C-SAM substrate with the hydrophobic lipid tails is 1–2 orders of magnitude more favorable in adhesion energy compared to the contact with the hydrophilic lipid heads, as modeled by our simulation of the DLPE/water/C-SAM system. It is very likely therefore that the difference in adhesion energy is the main factor that determines the preference of SLM over SLB on deposition of SUVs on C-SAM.

As the confinement was increased, both of the DLPE/water/SAM systems showed a monotonous decrease in the ensemble-average number of water molecules, $\langle N \rangle$. In this respect, they were similar to the symmetric O-SAM/water/O-SAM system but differed from the asymmetric O-SAM/water/C-SAM and symmetric C-SAM/water/C-SAM ones, where the function $\langle N \rangle(h)$ showed a discontinuity associated with capillary evaporation [14]. The lack of capillary evaporation in the DLPE/water/SAM systems is not surprising in view of a high water affinity of the DLPE bilayer due to an easy accessibility of its proton-acceptor and proton-donor groups to water molecules. A deep penetration of water into bilayer can be appreciated from snapshots of the DLPE/water/SAM systems in Figs. 5 and 6.

In conclusion, this work represents a first attempt to simulate an SLB as an open system, where confined water is allowed to exchange molecules with surrounding bulk water so as to sustain the chemical equilibrium with the latter. Compared to the previous GCMC simulations concerned with the short-range repulsion between phospholipid bilayers [11, 12] similar simulations of SLBs in the region responsible for adhesion are more demanding and inexact because of much smaller magnitudes of attractive pressure. This is particularly true of systems where the bilayer–substrate adhesion energy is less than 1 mJ/m^2.

Unfortunately, the experimental data on the adhesion forces operating in SLBs are limited by single systems [2, 31] so that our simulation results cannot be directly compared with experiment. Nevertheless, the acceptable agreement of our previous results for the SAM/water/SAM systems [14] with the experimental adhesion energies provides a reason to hope that the approach suggested in this and previous [14] works will be useful in predicting and interpreting the bilayer–substrate adhesion strength.

Acknowledgment This work was supported by the Deutsche Forschungsgemeinschaft through grant GR 625/60-1.

References

1. Sackmann ES (1996) Science 271:43–48
2. Anderson TH, Min Y, Weirich KL, Zeng H, Fygenson D, Israelachvili JN (2009) Langmuir 25:6997–7005
3. Heine DR, Rammohan AR, Balakrishnan J (2007) Molec Simul 33:391–397
4. Tarek M, Tu K, Klein ML, Tobias DJ (1999) Biophys J 77:964–972
5. Roark M, Feller SE (2008) Langmuir 24:12469–12473
6. Xing C, Faller R (2008) J Phys Chem B 112:7086–7094
7. Xing C, Faller R (2009) J Chem Phys 131:175104
8. Xing C, Ollila OHS, Vattulainen I, Faller R (2009) Soft Matter 5:3258–3261
9. Hoopes MI, Deserno M, Longo ML, Faller R (2008) J Chem Phys 129:175102
10. Różycki B, Weikl TR, Lipowsky R (2008) Phys Rev Lett 100:098103
11. Pertsin A, Platonov D, Grunze M (2005) J Chem Phys 122:244708
12. Pertsin A, Grunze M (2011) Curr Opin Colloid Interface Sci 16:534–541
13. Shelley JC, Patey GN (1994) J Chem Phys 100:8265–8270
14. Pertsin A, Grunze M (2012) J Chem Phys 137:054701
15. Smondyrev AM, Berkowitz ML (1999) J Comput Chem 20:531–545
16. Pertsin AJ, Hahn J, Grossmann H-P (1994) J Comput Chem 15:1121–1126
17. Williams DE (1967) J Chem Phys 47:4680–4684
18. Mar W, Klein ML (1994) Langmuir 10:188–196
19. Jorgensen WL, Maxwell DS, Tirado-Rives J (1996) J Am Chem Soc 118:11225–11236
20. Frenkel D, Smit B (2002) Understanding molecular simulation: from algorithms to applications, 2nd edn. Academic Press, San Diego
21. Allen MP, Tildesley DJ (1987) Computer Simulation of Liquids. Clarendon Press, Oxford
22. Jorgensen WL, Chandrasekhar J, Madura JD, Impey RW, Klein ML (1983) J Chem Phys 79:926–935
23. Pertsin AJ, Grunze M (1994) Langmuir 10:3668–3674
24. Nagle JF, Wiener MC (1988) Biochim Biophys Acta 942:1–10
25. Swendsen RH, Wang J-S (1987) Phys Rev Lett 58:86–88
26. Shelley JC, Patey GN (1995) J Chem Phys 102:7656–7663
27. Evans R, Marconi UMB (1987) J Chem Phys 86:7138–7148
28. Lingler S, Rubinstein I, Knoll W, Offenhäusser A (1997) Langmuir 13:7085–7091
29. Keller CA, Kasemo B (1998) Biophys J 75:1397–1402
30. Clear SC, Nealey PF (1999) J Colloid Interface Sci 213:238–250
31. Valtiner M, Donaldson SH Jr, Gebbie MA, Israelachvili JN (2012) J Am Chem Soc 134:1746–17543